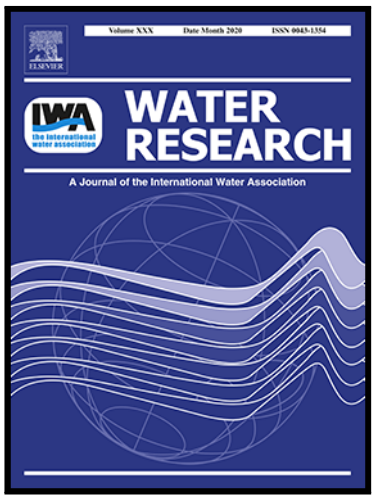

Urban rivers are hotspots of riverine greenhouse gas (N_2O, CH_4, CO_2) emissions in the mixed-landscape Chaohu Lake Basin

Wangshou Zhang , Hengpeng Li , Qitao Xiao , Xinyan Li

PII: S0043-1354(20)31159-3
DOI: https://doi.org/10.1016/j.watres.2020.116624
Reference: WR 116624

To appear in: *Water Research*

Received date: 12 August 2020
Revised date: 20 October 2020
Accepted date: 7 November 2020

Please cite this article as: Wangshou Zhang , Hengpeng Li , Qitao Xiao , Xinyan Li , Urban rivers are hotspots of riverine greenhouse gas (N_2O, CH_4, CO_2) emissions in the mixed-landscape Chaohu Lake Basin, *Water Research* (2020), doi: https://doi.org/10.1016/j.watres.2020.116624

Highlights:

- All studied rivers were acting as significant sources of atmospheric GHG
- Main factors governing riverine GHG production vary across rivers
- Urban rivers are emission hotspots of all greenhouse gases
- GHG mitigation measures should be more specifically targeted at urban rivers

Urban rivers are hotspots of riverine greenhouse gas (N_2O, CH_4, CO_2) emissions in the mixed-landscape Chaohu Lake Basin

Wangshou Zhang[1], Hengpeng Li[1*], Qitao Xiao[1], Xinyan Li[1]

[1]Key Laboratory of Watershed Geographic Sciences, Nanjing Institute of Geography and Limnology, Chinese Academy of Sciences, Nanjing 210008, China

*Correspondence to Hengpeng Li, Email: hpli@niglas.ac.cn

Abstract

Growing evidence shows that riverine networks surrounding urban landscapes may be hotspots of riverine greenhouse gas (GHG) emissions. This study strengthens the evidence by investigating the spatial variability of diffusive GHG (N_2O, CH_4, CO_2) emissions from river reaches that drain from different types of landscapes (i.e., urban, agricultural, mixed, and forest landscapes), in the Chaohu Lake basin of eastern China. Our results showed that almost all the rivers were oversaturated with dissolved GHGs. Urban rivers were identified as emission hotspots, with mean fluxes of 470 μmol m^{-2} d^{-1} for N_2O, 7 mmol m^{-2} d^{-1} for CH_4, and 900 mmol m^{-2} d^{-1} for CO_2, corresponding to ~14, seven, and two times of those from the non-urban rivers in the Chaohu Lake basin, respectively. Factors related to the high N_2O and CH_4 emissions in urban rivers included large nutrient supply and hypoxic environments. The factors affecting CO_2 were similar in all the rivers, which were temperature-dependent with suitable environments that allowed rapid decomposition of organic matter. Overall, this study highlights that better recognition of the influence that river networks have on global

warming is required—particularly when it comes to urban rivers, as urban land cover and populations will continue to expand in the future. Management measures should incorporate regional hotspots to more efficiently mitigate GHG emissions.

Keywords: Watershed; Chaohu Lake Basin; Carbon dioxide; Methane; Nitrous oxide; Urban

1. Introduction

Nitrous oxide (N_2O), methane (CH_4), and carbon dioxide (CO_2) are well-known greenhouse gases (GHG) (Raymond et al. 2013, Reay et al. 2012). Recent monitoring by the World Meteorological Organization showed that their concentrations in the global atmosphere have reached 331.1±0.1 parts per billion (ppb), 1,869±2 ppb, and 408.0±0.1 parts per million (ppm), steadily increasing by 123%, 259%, and 147% since the mid-18th century, respectively (WMO 2019). Such high atmospheric GHG enrichment has resulted in a number of issues, including global warming and associated ecological damages (Convey and Peck 2019). An Intergovernmental Panel on Climate Change (IPCC) report showed that global warming is likely to reach 1.5 °C in the next 10–30 years as GHG are continuously added to the atmosphere, which undoubtedly increases climate-related risks for natural and human systems (IPCC 2018). GHG emissions from various ecosystems have thus become one of the key issues in ecology and global change research (Raymond et al. 2013, Yvon-Durocher et al. 2014). Direct GHG production from terrestrial ecosystems as a result of intensified human activities has been well documented, and thus has become

a relatively well-constrained component of the global GHG budget (Quick et al. 2019). In contrast, GHG emissions from river networks have received less attention and are consequently less constrained, although studies have increasingly demonstrated that rivers play an important role in global GHG budgets that is disproportional to their areal extent (Borges et al. 2015b, Cole et al. 2007). Therefore, including more measurements of in-stream GHG emissions is essential to close knowledge gaps in both global and regional GHG assessment efforts as well as to gain a better understanding of the mechanisms behind riverine GHG production.

Forested, urban and agricultural rivers that drain different watershed landscapes result in different riverine dissolved GHG concentrations and fluxes (Borges et al. 2018, Mwanake et al. 2019). Of these, forested rivers were most frequently found to have low GHG emissions per unit area. For example, Borges et al. (2018) showed that forested rivers are important N_2O sources although their areal emissions were generally lower than agricultural rivers. They can also behave as N_2O sinks, as exhibited in some tropical forested rivers where DO levels were low and microbial conversion of N_2O to N_2 was strong, particularly when they are connected to wetlands (Borges et al. 2019). Audet et al. (2020) also observed source-sink dynamics of N_2O emissions in forested streams from Sweden. For CH_4 and CO_2, forested rivers are usually found to be significant atmospheric sources, as observed in the Amazon river (Amaral et al. 2018, Melack et al. 2004) and Congo river (Borges et al. 2015a). Such differences among GHG types and across regions underscores the complexity of GHG emissions from forested rivers, implying the necessity of more regional-specific GHG

measurements.

In contrast to emissions from forested rivers, GHG emissions from agricultural rivers have received more attention, ranging from low-order headwater streams (Outram and Hiscock 2012, Schade et al. 2016, Wilcock and Sorrell 2008) to high-order rivers (Turner et al. 2015, Xia et al. 2013). These studies consistently documented the significance of GHG emissions from agricultural streams and rivers, largely due to high inputs from surface runoff and groundwater recharge as well as strong in-stream GHG production (Laini et al. 2011, Qin et al. 2020, Xia et al. 2013). The main controls are dependent on riverine physical and chemical conditions, including carbon and nitrogen (N) availability, temperature, dissolved oxygen (DO), and pH (Quick et al. 2019, Stanley et al. 2016). A growing number of studies focusing on agricultural rivers have improved the methods for regional- and global-scale GHG budget accounting (Tian et al. 2019, Wallin et al. 2014), while also drawing more attention to refined agricultural practices designed to better mitigate GHG emissions (Mwanake et al. 2019, Peterson et al. 2001).

Urban-impacted river networks, however, receive less attention, though they are fed by treated and untreated sewage and their GHG emissions are sometimes substantial. Existing studies on urban rivers were mainly focused on their spatial and temporal patterns of GHG emissions, the influences of sewage discharge and damming (e.g., Jin et al. (2018), Li et al. (2020), Wang et al. (2020)). For example, several studies documented that the highest GHG (N_2O, CH_4, CO_2) emissions were

often observed in rivers surrounded by highly urbanized regions (e.g., He et al. (2017), Wang et al. (2020), Wang et al. (2018) and Yu et al. (2013)). Their areal GHG emissions can be several to tens of times those reported in nearby less-urbanized rivers. Similarly, a parallel analysis of the sewage-draining river sections also indicated that their GHG emissions were up to 10 times higher than the river sections without sewage discharge (Hu et al. 2018). Other studies discerned that damming on urban rivers had an amplifying effect on GHG emissions (Jin et al. 2018, Yang et al. 2020). Overall, GHG emissions from urban rivers are higher than those of forested rivers. In many circumstances, urban river emissions appear to be even higher than those of zero-order agricultural streams, which are widely accepted as GHG emission hotspots (Liu et al. 2019, Smith et al. 2017). These studies consistently support a growing awareness that urban-impacted rivers are likely greenhouse gas emission hotspots.

However, surface water emissions of CO_2, CH_4, and N_2O have rarely been determined basin-wide in river systems that drain different watershed landscapes. The compiled data from different rivers across the world (as shown in Table 1S) suggested that GHG fluxes from some agricultural and forested rivers were even higher than most of the urban rivers, showing that the roles of the specific river types in contributing GHG fluxes are unclear. This points to the need for more careful investigations on GHG emissions from different rivers. Moreover, current bottom-up GHG budget accountings mainly emphasize agricultural and forested rivers (e.g., Audet et al. (2020), Iurii et al. (2014), Melack et al. (2004), Reay et al. (2012), and

Tian et al. (2019)), with poor considerations of urban rivers, although urban rivers could contribute even higher GHG emissions. This further underscores the necessity of more reasonable specifications on GHG emissions from urban rivers. In the future, as urban land and population continue to expand, the associated contributions of GHG to climate forcing will undoubtedly increase. Thus, quantification of the magnitudes and controls of GHG fluxes from urban rivers is critical to comprehensively understand global climate change processes and formulate GHG mitigation strategies for sustainable development.

This study determined whether urban rivers behave as regional hotspots of diffusive greenhouse gas (N_2O, CH_4, CO_2) emissions as compared to other river types. Here, the urban rivers drain watersheds with > 20% of the urban area. We measured riverine dissolved N_2O, CH_4, and CO_2 concentrations in 95 different river reaches in the mixed-landscape Chaohu Lake basin of eastern China; 19 of the reaches represented urban rivers. The remaining 21, 18, and 37 reaches were agricultural, forested, and mixed river reaches. All GHG data were obtained following the same sampling, storage, and measurement protocols, which allowed us to focus on the differences in GHG emissions between the rivers in a comparable way. In addition to addressing the overall scientific question, this study also aimed at answering the following specific questions:

1) What are the magnitudes and patterns of GHG concentrations in river networks in a mixed-landscape basin?
2) What riverine physical and chemical conditions are influencing riverine GHG

saturation?

3) What are the controls of the spatial variabilities of GHG emissions among rivers?

2. Materials and methods

2.1 Study area and sampled riverine types

Chaohu Lake is the fifth-largest freshwater lake in China (Fig. 1), with a surface area of ~780 km^2 and a basin area of ~13,500 km^2. It lies on the north shore of the lower reaches of the Yangtze River, and is adjacent to the highly developed and densely populated Yangtze River delta. The lake is mainly fed by 33 rivers, but only a few (e.g., the Nanfei and Hangbu rivers) contribute most of the water. The population in the basin has reached 10.2 million, most of which is concentrated in the highly urbanized northern area.

To reveal the magnitudes and their controls of GHG emissions, we measured dissolved GHG concentrations in 95 river reaches in the Chaohu Lake basin. To further compare the GHG emission differences among rivers, we separated the river reaches into different types—i.e., urban, agricultural, forested, and mixed river reaches. The distinctions were made according to the landscape compositions in the watersheds, which drained into these sampled sites. Here, the four types—forested watersheds (forests > 50%), agricultural watersheds (cropland > 60%), urban watersheds (urban > 20%), and mixed watersheds (forest ≤ 50%, cropland ≤ 60%, and urban ≤ 20%)—were sorted and their mainstems were defined as corresponding riverine types (Zhang et al. 2020). The cutoff percentages used to establish the river

classification sought a compromise between accurate classification of river type and local landscape composition to better balance the collected data to ensure that each group had a similar number of datasets. Thus, though our classification may not be precise, it is adequate to test our hypothesis that urban rivers are hotspots of riverine GHG emission.

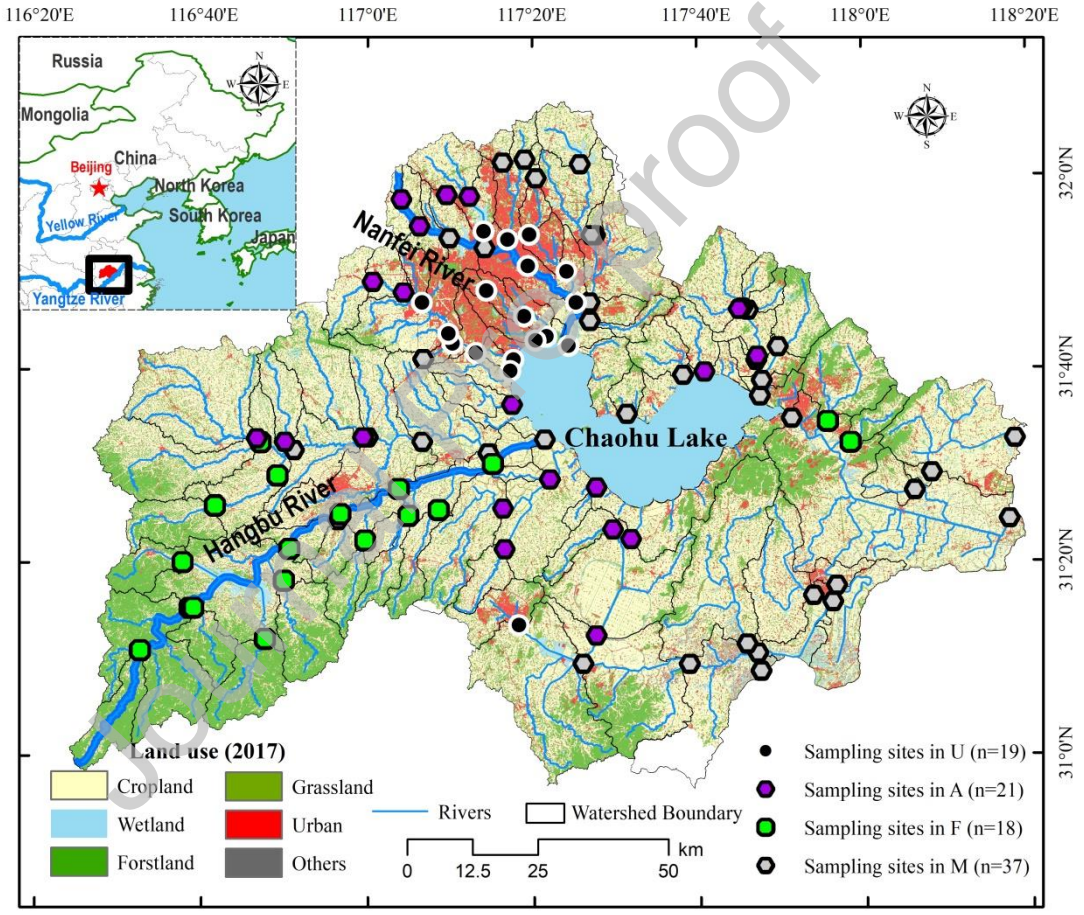

Figure 1. Sampling stations and land cover in the Chaohu Lake basin. To determine the differences in GHG emission among rivers, we grouped 95 river reaches, where the samples were obtained, into four types: urban (U), agricultural (A), forested (F), and mixed (M) rivers, according to the main landscape compositions in their drainages.

2.2 Sample collection and analysis

Samples were collected from 95 sites throughout the Chaohu Lake basin at bimonthly intervals between February 2018 and December 2018, so that six visits were made to each site and 570 samples were collected in total. Of the 95 sites, 19, 21, 18, and 37 of them were collected from river reaches in urban, agricultural, forested, and mixed watersheds, respectively. For each sampling visit, water samples were collected at a depth of 20 cm below the water surface from bridges using a Niskin bottle. Subsamples for N_2O and CH_4 analysis were then transferred into borosilicate serum bottles (135 ml). Several volumes were allowed to overflow, and a 0.2 ml saturated $ZnCl_2$ solution was added to stop microbial metabolism. The sample bottles were sealed with a rubber septum with no headspace or bubble, and stored underwater at 4 ℃ during the transportation but kept at ambient temperature ~12 hours before analysis. Subsamples for CO_2 analysis were obtained using polypropylene syringes. Three 50 mL syringes were used to take 25 ml water samples with a mix of 25 mL air of known CO_2 concentration and gently shaken for 5 min to allow for equilibration under in-situ conditions. The headspace volume (25 mL) was then transferred into a new gastight syringe and carefully preserved to avoid gas leakage. More details about this can be found in Dalsgaard et al. (2000) and Teodoru et al. (2015). We also collected 600 ml of surface water at each sampling site using a polyethylene bucket to measure water quality concentrations, including total nitrogen (TN), ammonia-nitrogen (NH_4-N), nitrate-nitrogen (NO_3-N), nitrite-nitrogen (NO_2-N), total phosphorus (TP), and the permanganate index of chemical oxygen demand (COD).

Gaseous samples for N_2O and CH_4 analysis were obtained from the headspace of a glass bottle (135 mL) filled with 85 mL of water, tightly capped, and shaken vigorously for 5 min to reach gas equilibrium between the headspace and water phase. The headspace was created using 50 mL ultra-pure N_2 following the headspace equilibration technique (Dalsgaard et al. 2000). Ten milliliters of the headspace gas, as well as the CO_2 samples in the syringes, were separately drawn out and injected into a gas chromatograph (7890 B, Agilent Technologies, Santa Clara, California, USA) configured with electron capture (ECD) and flame ionization (FID) to obtain GHG concentration data. The precolumn and analytical columns were 1.8 m and 3.6 m long-steel columns packed with HayeSep Q (80/100 mesh). A standard gas mixture of known N_2O (2.07 ppm), CH_4 (0.513 ppm), and CO_2 (409 ppm) concentrations was adopted for calibration. The detection limit of N_2O, CH_4, and CO_2 is 0.014 ppm, 0.011 ppm, and 0.089 ppm, respectively. And the corresponding reproducibility of measurements was ±2.8 %, ±5.8 %, and ±5.1%, respectively.

The in-situ GHG concentrations in water were then calculated based on their corresponding solubility at laboratory temperature and pressure vs. in-situ temperature and pressure (Wanninkhof 1992, Weiss and Price 1980). For the laboratory determinations of the water quality indicators, the 0.7 μm filtered water samples were used to analyze the dissolved forms of nutrients (i.e., NH_4-N, NO_3-N, and NO_2-N), and the raw water samples were used for measuring TN, TP, and COD concentrations. All of these water quality indicators were analyzed following standard protocols (MEP 2002).

In-situ physical and chemical indicators such as water temperature (Temp), dissolved oxygen (DO), specific conductance (SPC), oxidation-reduction potential (ORP), chlorophyll a (Chl-a), fluorescent dissolved organic matter (fDOM), and turbidity were measured by a YSI 6000 Multiprobe field meter. Riverine attributes such as width, depth, and mean flow rates at all sampling riverine reaches were obtained independently for each sampling visit by a boat-mounted Acoustic Doppler Current Profiler (ADCP), RiverSurveyor M9 (SonTex, San Diego, CA, USA).

2.3 Data calculations

The percentage saturation of GHG in the water samples was calculated as:

$$GHG\ saturation = \left(\frac{C_w}{C_{eq}}\right) \times 100\% \quad (1)$$

where C_w is the measured GHG concentration in water measured by the headspace equilibration method described in Section 2.2. C_{eq} is the corresponding equilibrium GHG concentration in river water that is in equilibrium with the ambient atmosphere at the in-situ pressure and temperature. The methods of obtaining C_{eq} for N_2O, CH_4, and CO_2 can be found in Weiss and Price (1980), Wiesenburg and Guinasso (1979), and Weiss (1974), respectively.

The diffuse fluxes of GHG (F, μmol m^{-2} d^{-1} -N_2O, mmol m^{-2} d^{-1} -CH_4, or mmol m^{-2} d^{-1}-CO_2) at the interface of the river and the atmosphere were calculated as:

$$F = k \times \left(C_w - C_{eq}\right) \quad (2)$$

where k is the integrated gas transfer coefficient (m s^{-1}) for GHG that incorporates

physical processes. The coefficient *k* was calculated as (Clough et al. 2007):

$$k = \sqrt{\frac{DU}{h}} + 2.78e^{-6}\alpha u_{10}^{2}\left(\frac{S_c}{660}\right)^{0.5} \quad (3)$$

where $\sqrt{\frac{DU}{h}}$ is the water current term, which was calculated using the river water velocity (*U*; m s^{-1}), average river depth (*h*; m), and a diffusion coefficient for each gas in the water (D; m^2 s^{-1}). $2.78e^{-6}\alpha u_{10}^{2}\left(\frac{S_c}{660}\right)^{0.5}$ is a wind term. $2.78e^{-6}$ is a unit conversion factor (cm h^{-1} to m s^{-1}), α is a constant (0.31), and u_{10} is the wind speed at a height of 10 m above the river. S_c is the Schmidt number for the corresponding gas, which can be obtained from Wanninkhof (1992).

River depth and water velocity data were derived from in-situ measurements for each sampling visit, as described in Section 2.2. The diffusion coefficient for each of the gases was derived from Jähne et al. (1987). The wind speed data (u_{10}) was obtained from nearby weather stations, which are available from the China Meteorological Data Service Center (http://data.cma.cn/en).

In addition, other methods, such as those in Raymond et al. (2012), have been applied to obtain gas transfer coefficients (*k*) (Audet et al. 2017, Borges et al. 2019, Wang et al. 2020). To evaluate the influences of different methods of *k* on the estimated fluxes, we provide two datasets of GHG fluxes that were derived from the empirical models: Ray01 (Eq. (1) in Raymond et al. (2012)) and Ray05 (Eq. (5) in Raymond et al. (2012)). Ray01 predicts *k* as a function of the slope (*S*; unitless), stream velocity (*U*; m s^{-1}), and depth (*h*; m) at sampling time while Ray05 is only based on *S* and *U* (Raymond et al. 2012). More details about the methods and

estimated results can be found in the supplementary material.

2.4 Data analysis

Statistically significant differences in GHG saturation, fluxes, and water physical and chemical indicators among rivers were determined using the one-way analysis of variance (one-way ANOVA). The Pearson correlation was calculated first to determine the level of correlation between riverine physical and chemical parameters and GHG saturations. A stepwise multiple linear regression was used to further explore the relative importance of riverine physical and chemical parameters in explaining the spatial-temporal variability of GHG saturation. The normality of the parameters was tested using the Kolmogorov-Smirnov test. If the data did not follow a normal distribution, log-transformed parameters were applied. The adjusted R^2 of the model was used to evaluate the explanatory power of the variable. Intervariable collinearity of the regression models was diagnosed by referring to the variance inflation factor (VIF); a variable with a VIF > 5 was considered strong collinearity with other variables and was discarded. All of these statistical tests were performed with SPSS, Version 19.0 (IBM Corp., 2010), a statistical product and service solution software.

The spatial distributions of GHG concentration and fluxes were exhibited using the ArcGIS Desktop software (Version 10.3, ESRI, 2014). To identify the regions with the greatest diffusive GHG emissions, we applied hotspot analysis using the “Hot Spot Analysis (Getis-Ord Gi*)” tool in GIS. The analysis is a screening tool focusing

on the locations of abundant phenomena (Nelson and Boots 2010), which is suitable for discerning cluster structures of high (hotspot) or low (cold spot) values. This method has been intensively used in analyzing spatial patterns of environmental data (Jana and Sar 2016, Zhang et al. 2019). More details of this method can be found in Mitchell (2005).

3. Results

3.1 Riverine physical and chemical characteristics

The overall physical and chemical characteristics of the different rivers are presented in Table 1 with mean values and their standard deviations (SD). Riverine characteristics in urban rivers differed significantly from other rivers. The differences mainly included higher TN, TP, SPC, fDOM, and Chl-a concentrations, and lower pH and DO contents. On average, TN and TP concentrations in the urban rivers reached 7.7 and 0.5 mg L^{-1}, respectively, which is > 3 times of those in non-urban rivers. NH_4-N was one of the main N forms, accounting for 40% of TN in urban rivers, in contrast to its minor percentages in other rivers. Significant nutrient enrichment in urban rivers, along with their relatively high SPC, COD, fDOM, and Chl-a, indicate that local urban rivers are polluted by intensive domestic and industrial sewage discharges.

In contrast, concentrations of TN, TP, and other nutrient-related indicators in non-urban rivers were lower, with most of the lowest concentrations recorded in less-disturbed forested rivers. The mean contents of TN and TP in forested rivers

reached 1.72 mg L and 0.11 mg/L. DO levels in forested rivers (9.7 mg/L) indicated aerobic environments. Concentrations of main indicators in the agricultural and mixed rivers often fell between those in urban and forested rivers, with some exceptions—for example, COD was highest in agricultural rivers.

Table 1. Statistical characteristics of riverine physical and chemical indicators.

3.2 Variability of GHG concentrations

Riverine dissolved GHG (N_2O, CH_4, CO_2) concentrations for different rivers are presented in Fig. 2. All of their mean concentrations had strong spatial variabilities, which spanned up to three orders of magnitude. Even so, most of the dissolved concentrations (>99%) were far above the theoretical water–atmosphere equilibrium values, indicating significant oversaturation of GHG in the rivers studied here.

Averaged concentrations of riverine GHG can be ranked as: urban rivers > mixed rivers > agricultural rivers > forested rivers. GHG concentrations in urban rivers were among the highest, with mean concentrations of 408 nmol L^{-1}, 5.5 μmol L^{-1}, and 671 μmol L^{-1} for N_2O, CH_4, and CO_2, respectively. These values correspond to 4.1~9.7, 9.1~17.6, and 1.4~2.9 times of those in non-urban rivers. One-way ANOVA further demonstrated that GHG contents in urban rivers were significantly larger than others. The parallel analysis did not always determine significant differences between agricultural and mixed rivers, but their GHG contents were higher than forested rivers.

Fig. 3 shows the spatial patterns of the gas concentrations, illustrating the

similarity between the gases. The relatively high dissolved concentrations were always observed in the rivers nearby or within urban regions, while the low concentrations were mainly found in the southwestern rivers draining from forested-dominant landscapes. Along rivers, there were visible upstream-to-downstream patterns, which may be related to the spatial heterogeneity of the landscapes. For example, the maps of the spatial distributions of GHG in highly urbanized regions show that, along the same reaches (e.g., the Nanfei River as shown in Fig. 3), the GHG levels were relatively low in the upstream, but as the rivers passed through urbanized regions, GHG contents became high. The coefficient of variation (C.V.) of GHG contents differed among the rivers. A higher C.V. in urban rivers suggests stronger temporal variabilities of GHG production.

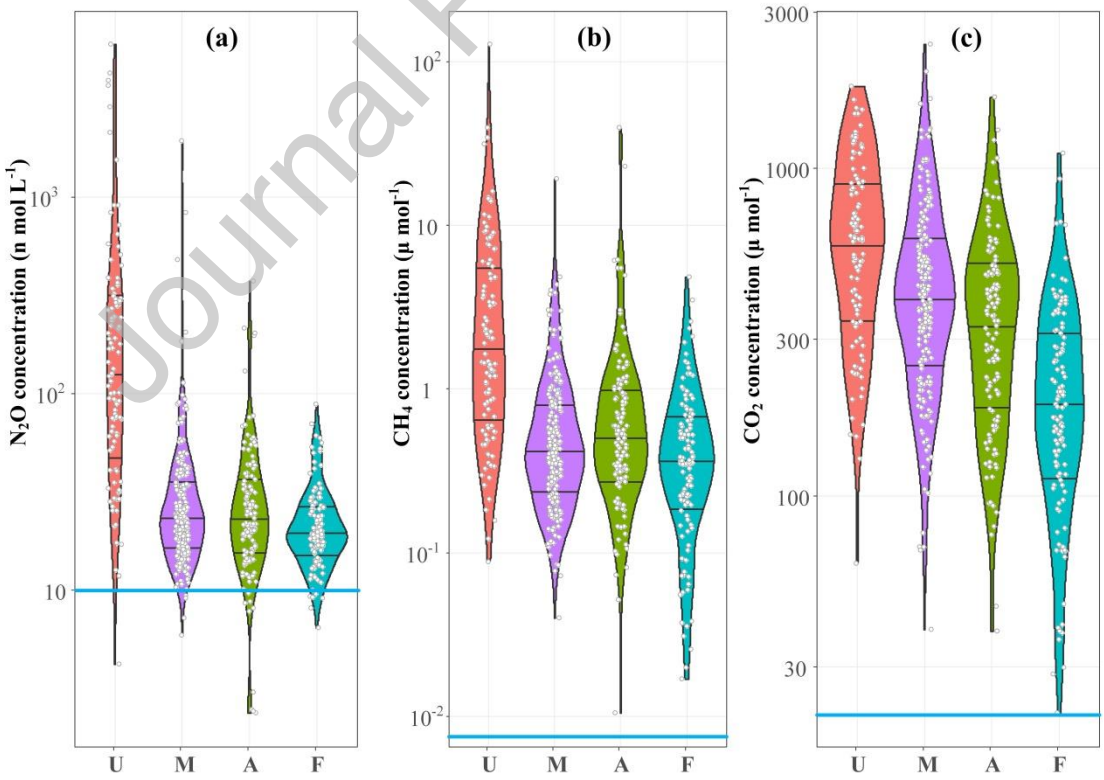

Figure 2. Violin plot summaries of (a) N_2O, (b) CH_4, and (c) CO_2 concentrations for

all water samples from the four river types. The three horizontal lines inside each of the boxes denote 25%, 50%, and 75% quantiles. The light-blue horizontal lines in each box show their mean saturation concentrations of the dissolved gas for all of the samples.

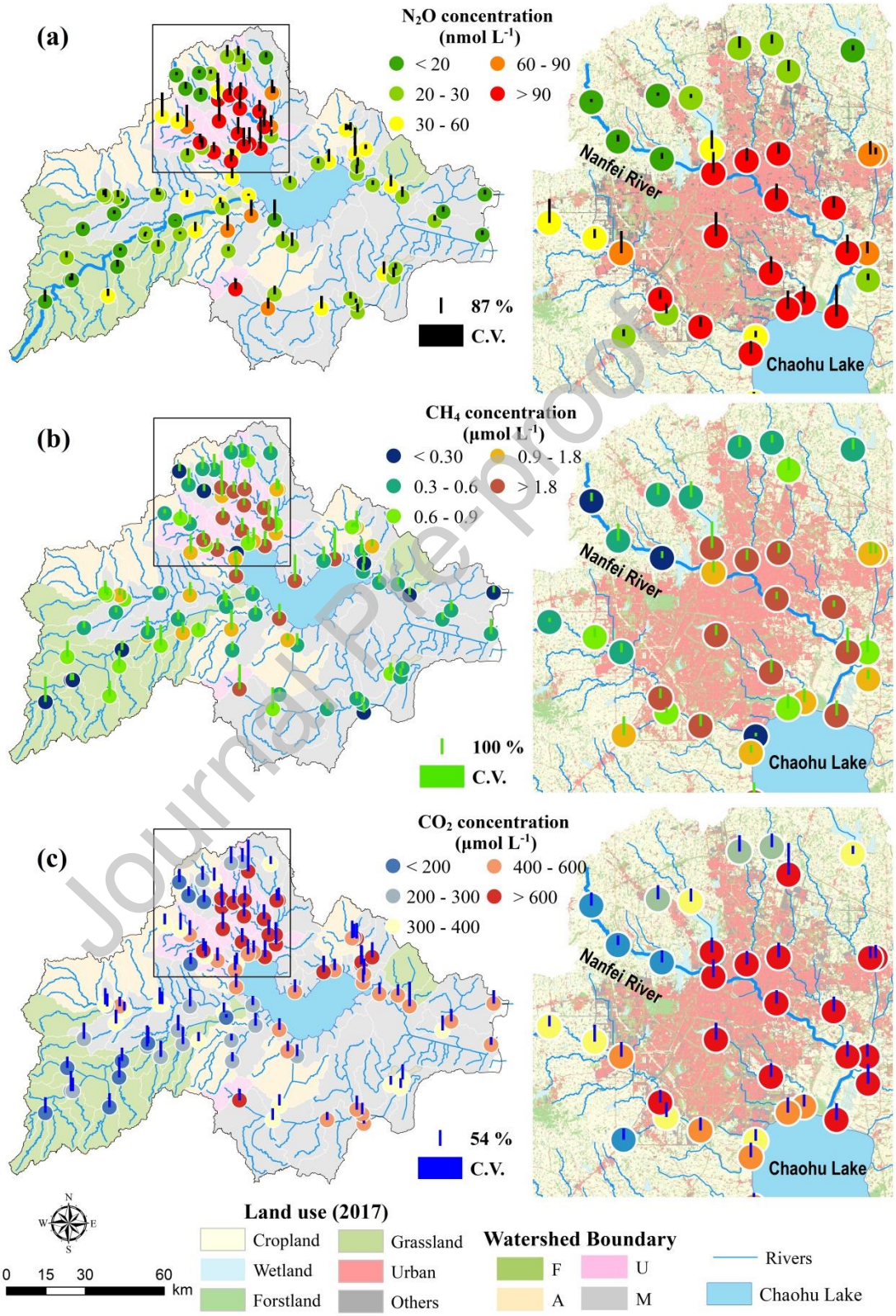

Figure 3. Spatial distributions of (a) N_2O, (b) CH_4, and (c) CO_2 concentrations at all 95 sites in Chaohu Lake basin. Right panel is maps of the corresponding GHG concentrations in rivers from the urbanized region.

3.3 Influences of environmental factors

To discern potential controls of GHG production, we analyzed the correlations between each of the environmental variables and GHG saturation. As shown in Fig. 4, it is evident that the physical and chemical indicators have different relationships with GHG saturation among rivers.

In the urban rivers, fDOM, a proxy of dissolved organic matter in rivers, was most significantly related to N_2O saturation. In the rivers with less N enrichment, such as forested and mixed rivers, N-related indicators (e.g., NO_3-N and TN) became the main explanatory variables. Meanwhile, in the forested rivers, DO was highly related to N_2O saturation.

For CH_4, the indicators TN, NH_4-N, TP, and COD were positively related to its saturation in urban rivers. The parallel relationships were also determined in agricultural and mixed rivers, but water temperature in these rivers was found to be more significantly related to CH_4. In forested rivers, NO_3-N was negatively related to CH_4 saturation.

As for CO_2, both Chl-a and conductivity (i.e., SPC) were positively related to its saturation across the different rivers. Many of other factors (e.g., N-related indicators) that were correlated to CO_2 in urban rivers, have not shown any relationship with CO_2 in agricultural and forested rivers, suggesting the different mechanisms of riverine

CO_2 production among rivers.

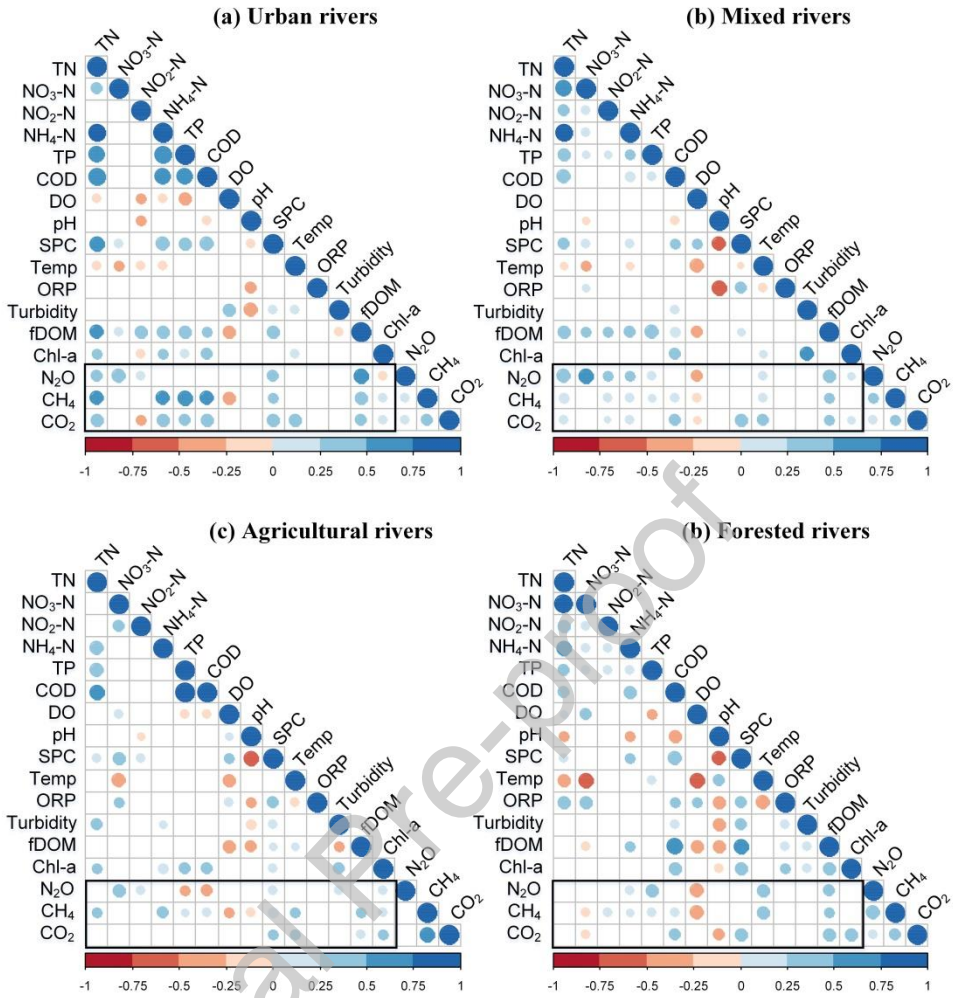

Figure 4. Matrices of Pearson correlations between riverine physical and chemical variables and the saturation of each greenhouse gas (black rectangles) in (a) Urban rivers, (b) Mixed rivers, (c) Agricultural rivers, and (d) Forested rivers. Red and blue dots inside the squares correspond to the negative and positive correlations with $p > 0.05$, respectively. Light-colored small dots represent low correlations while darker-colored large dots correspond to higher correlations. Missing dots inside the squares indicates an insignificant relationship between the pairwise variables.

3.4 Diffusive GHGs emission fluxes

The mean estimated diffusive N_2O, CH_4, and CO_2 emission fluxes (mean ± SD) from Chaohu Lake basin rivers was 115.3 ± 496.8 μmol m^{-2} d^{-1}, 2.3 ± 8.3 mmol m^{-2} d^{-1}, and 574.5 ± 597.3 mmol m^{-2} d^{-1}, respectively. Urban river reaches were found to

have the highest N_2O, CH_4, and CO_2 fluxes, with a mean value of 471.2 ± 1048.8 μmol m^{-2} d^{-1}, 7.1 ± 17.2 mmol m^{-2} d^{-1}, and 895.7 ±780.0 mmol m^{-2} d^{-1}, equivalent to ~14, seven, and two times that of the non-urban rivers, respectively (Table 2). Mixed rivers emitted the second-highest gas fluxes, except for CH_4, which was only ~ 50% of that in agricultural watersheds. As expected, forested rivers emitted the lowest GHG fluxes among the rivers. However, flux estimations using Clough et al. (2007) may be conservative, especially compared with the methods from Raymond et al. (2012) (see Fig. 1S). The estimated fluxes for the rivers of the Chaohu Lake basin using Ray01 and Ray05 were 195.5 ±1847.0 and 206.0 ±951.3 μmol m^{-2} d^{-1} for N_2O, 2.1 ± 7.9 and 3.9 ± 13.3 mmol m^{-2} $d^{-1}$for CH_4, and 584.5 ± 1455 and 1007.4±919.1 mmol m^{-2} d^{-1} for CO_2, respectively.

Table 2. Diffusive emissions of greenhouse gases and their CO_2-equivalent fluxes from different rivers.

Using the global warming potential (GWP) factor for N_2O of 265 CO_2-equivalent and CH_4 of 28 CO_2-equivalent for a 100-year time horizon (IPCC 2014), the mean GHG fluxes in the Chaohu Lake basin's river network was translated to the CO_2-equivalent flux of 27.6 g CO_2 m^{-2} d^{-1}. CO_2 was the main contributor to the riverine GWP, with N_2O and CH_4 contributing only 5% and 4%, respectively, to the 100-year GWP. Urban rivers had the largest CO_2-equivalent fluxes across the rivers, about 1.8~3.4 times that of the other rivers. The CO_2-equivalent fluxes in urban rivers using Ray01 and Ray05 were 53 and 85 g CO_2 m^{-2} d^{-1}, which were 1.7~3.2 times and 2.0~2.9 times of those in the other rivers, respectively (as shown in Fig. 1S).

Fig. 5 shows the GHG fluxes for urban, mixed, agricultural, and forested rivers. The fluxes of all the gases had clear spatial patterns, with relatively low GHG fluxes in the upstream headwaters and high fluxes in the downstream. Along a river, GHG fluxes tended to increase when the river passed through urbanized or agricultural regions. That spatial pattern is most clearly exhibited in two contrasting rivers: the Hangbu River and the Nanfei River, which mainly drain agricultural and urban landscapes, respectively. Along both of those rivers, there were visible trends of increasing GHG fluxes along their upstream-to-downstream continuums. But this pattern was more explicitly observed in the urban-impacted Nanfei River.

Further hotspot analyses showed that 20, 11, and 9 sites clustered in or adjacent to the urban region were identified as emission hotspots of N_2O, CH_4, and CO_2 at the 90% confidence level, respectively (as shown in Figs. 5b, 5d, and 5f). Specifically, two sites in agricultural rivers were also identified as CO_2 hotspots, suggesting that agricultural rivers also may be prone to contribute significant CO_2 fluxes. Agricultural rivers also had CO_2 cold spots (see Fig. 5f), indicating a strong spatial heterogeneity across agricultural rivers. As expected, 7 out of 18 sites that sampled forested rivers were identified as CO_2 cold spots. This agrees with established knowledge that forested rivers are normally subject to less CO_2 production. Parallel cold spots for N_2O and CH_4 were not determined for forested rivers or other types of rivers, which also agrees well with previous findings that forested rivers could be important sources for regional N_2O and CH_4 emissions (Audet et al. 2020, Melack et al. 2004). The parallel estimations using Ray01 and Ray05 had similar spatial patterns of GHG

hotspots (see Figs. 2S and 3S). Therefore, all of the methods support the assertion that urban rivers are the GHG hotspots, although their magnitudes of the estimated fluxes were different.

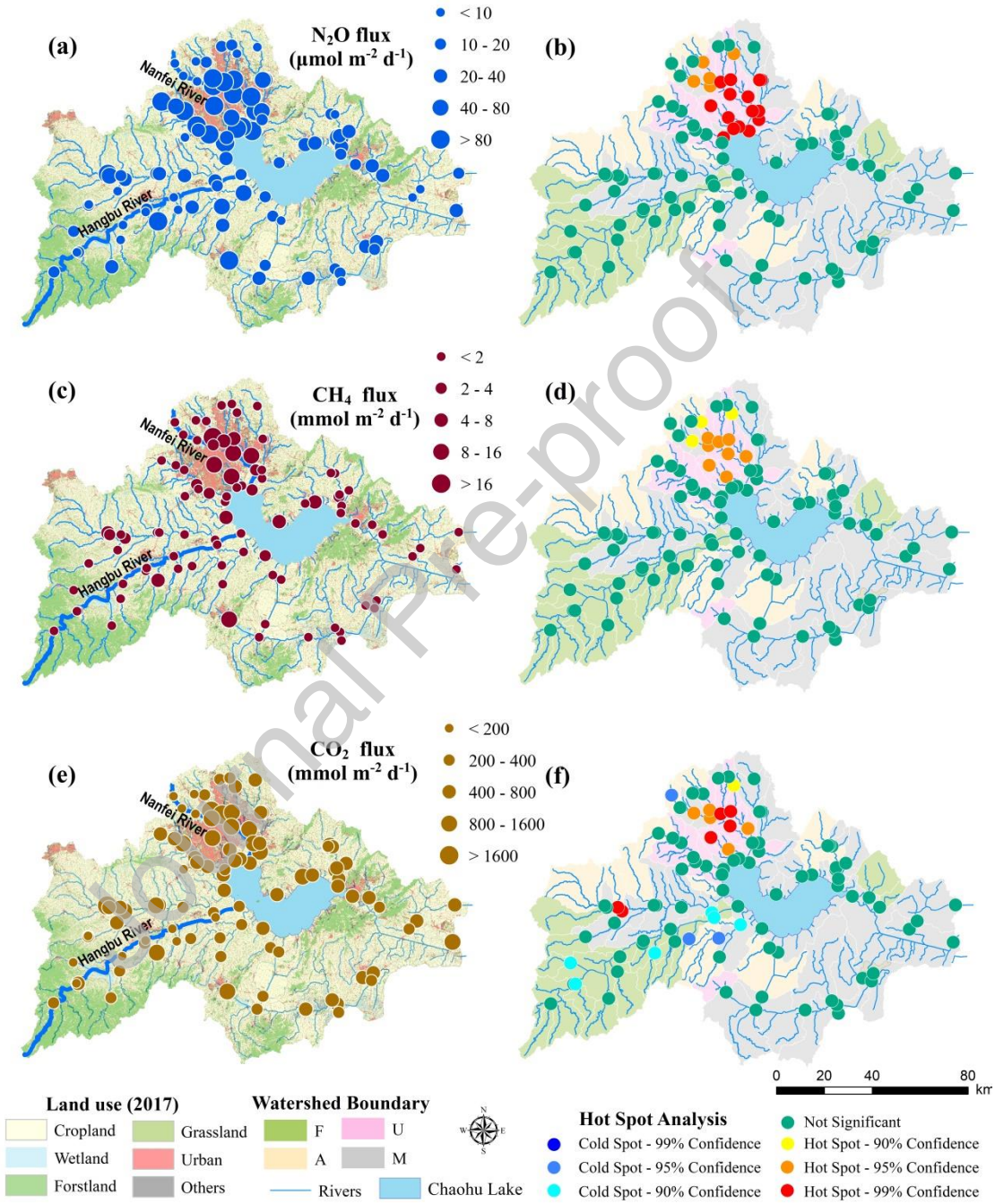

Figure 5. Spatial characteristics of (a) diffusive N_2O flux, (b) hotspots of N_2O emissions, (c) diffusive CH_4 flux, (d) hotspots of CH_4 emissions, (e) diffusive CO_2 flux, and (f) hotspots of CO_2 emissions.

4. Discussion

4.1 The roles of riverine physical and chemical factors

Mean N_2O, CH_4, and CO_2 saturations in the river networks of the Chaohu Lake basin reached ~1000%, 60000%, and 2900%, respectively. Such high riverine GHG saturations may be highly associated with biogenic processes, including incomplete denitrification (Quick et al. 2019), methanogenesis (Cotovicz et al. 2016, Stanley et al. 2016), and respiration (Humborge et al. 2010, Sobek et al. 2005). Any factors that are direct or indirectly involved in these processes could be their potential proximate controls. As expected, many riverine factors including availability of carbon (as represented by fDOM and COD) and nitrogen (e.g., NO_3-N, NH_4-N), DO, temperature, SPC, and pH have relationships with GHG saturations (see Fig. 4). Among them, nutrient-related indicators (e.g., TN, NO_3-N, NH_4-N, fDOM, and COD) were most significantly correlated, suggesting the importance of nutrient supply in promoting GHG production (Laini et al. 2011, Turner et al. 2016). The findings match those observations in other aquatic ecosystems, including inland rivers (Borges et al. 2015b, Raymond et al. 2013), lakes (Cunada et al. 2018, Davidson et al. 2015), and coastal bays (Cotovicz et al. 2016).

DO is another important factor related to gas production, as the associated functional microorganisms are usually facultative aerobes or obligate anaerobes (Marescaux et al. 2018, Quick et al. 2019). Thus, it is not surprising to observe that N_2O and CH_4 saturations were negatively correlated to DO in oxic forested rivers (Fig.

4). In general, N_2O production was usually favored under suboxic conditions, a suitable environment for coupled nitrification-denitrification (Ji et al. 2015, Wrage et al. 2001), which allows denitrifiers to obtain NO_3-N through aerobic nitrification leading to N_2O production (Quick et al. 2019). In the urban rivers studied here, mean DO level reached 6.4 mg/L, which can be characterized as suboxic conditions. Thus, the optimal DO condition for N_2O production could be obtained (Quick et al. 2019), and small variations of DO (as indicated by its low SD in Table 1) can hardly become an important control. Unlike that of N_2O, CH_4 production usually prefers anaerobic conditions (Stanley et al. 2016). Therefore, the two gases can react differently to DO variations in some settings (e.g., in urban rivers, see Fig. 4). If we now turn to CO_2 saturation, we find that SPC is an important influential factor. High SPC usually indicates a river water's greater ability to conduct electrical current, which may imply a more suitable condition for the rapid decomposition of organic matter for microbial production (Quick et al. 2019). High SPC may also indicate more contributions of water and dissolved gases from groundwater recharge or wastewater, as their conductivity could be higher. The most surprising aspect of the data is in the positive relationships between CO_2 saturation and Chl-a, which is contrary to established knowledge that primary producers (represented by Chl-a) usually deplete riverine CO_2 to build biomass (Davidson et al. 2015, Xiao et al. 2020). It should be documented that Chl-a was measured by a YSI Multiprobe field meter, which can be influenced by light and some substances that have similar fluorescent properties with those of Chl-a. Thus, in the spatial dimension, high Chl-a may indicate high presences of algae and

bioavailable substances that may favor CO_2 production.

Our data showed that GHG levels are also related to water temperature, with exceptions of N_2O and CH_4 in urban rivers. The results challenge the established empirical evidence for temperature dependence on riverine microbial production (Davidson et al. 2015). These results are perhaps not surprising, as thermal influence does not act in isolation in any ecosystem and can be concealed by more important factors when these factors also correlate with water temperature (Stanley et al. 2016). For example, Borges et al. (2015) analyzed 12 different basins across a whole continent of Africa, and found that connectivity with wetland landscapes was a more important factor than temperature in tropical regions. In our study, it is clear that N-related indicators were usually negatively related to water temperature (see Fig. 4), and thus the variability in nutrient supply may have overwhelmed temperature controls on microbial metabolisms, with the net result that the GHG saturations missed the linkage with water temperature.

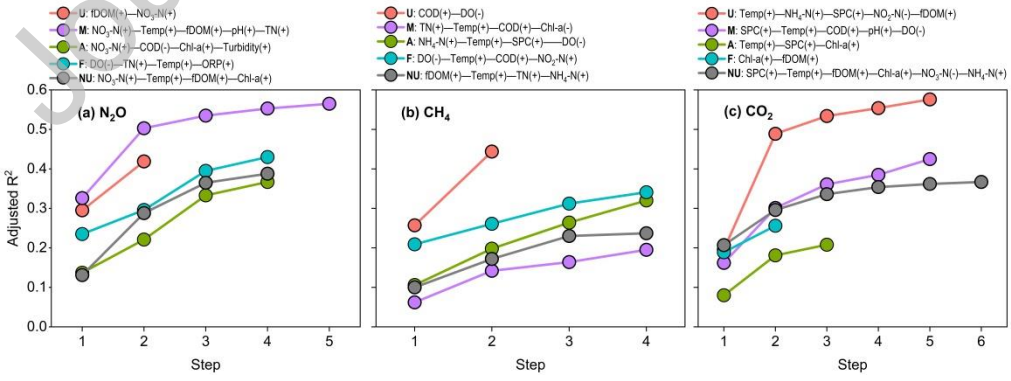

Figure 6. A stepwise multiple regression analysis with log-transformed (a) N_2O, (b) CH_4, and (c) CO_2 saturation as the dependent variable. We used 114, 126, 108, 222, and 456 pairwise data obtained from urban, mixed, agricultural, forested, and non-urban (NU, mixed+agricultural+forested) rivers, respectively, to perform each of

the regressions. The final set of model predictors in each regression is shown in sequence, with an order of their relative importance in explaining the dependent variables. Note that '+' and '-' in the brackets denote positive and negative relationships between predictor and GHGs saturation, respectively.

To better discern differentiated controls of GHG saturation among rivers, we performed a stepwise regression analysis. As shown in Fig. 6, the considerable differences in the explanatory power of the stepwise regressions and associated predictors reflect multiple controls on the production of GHG among rivers. For N_2O, around 37%~57% of the spatial and temporal variabilities can be explained by variables, including fDOM, NO_3-N, COD, DO, and temperature. This demonstrated that N_2O production is mainly sensitive to nutrient supply and DO (He et al. 2017, Mwanake et al. 2019, Wang et al. 2015). However, controls of N_2O saturations differed among rivers. For example, in the N-enriched urban rivers, N_2O production could be limited by unmatched supplies of electron donors (e.g., organic carbon) with respect to that of N (see Table 1). This was supported by the highest explanatory power of the proxy of the carbon sources (i.e., fDOM) in explaining the variations of N_2O saturation. In the less N-enriched mixed and agricultural rivers, however, N_2O saturation is most significantly explained by NO_3-N. And in the forested rivers, DO become the most significant limiting factor, suggesting that DO is the primary control of N_2O production in oxygen saturated environments (Venkiteswaran et al. 2014).

In comparison to N_2O, fewer variations in CH_4 saturation (20~44%) can be explained by the physical and chemical indicators. The fuel for respiration (i.e., organic matter) was the main control of CH_4 production throughout the rivers as

indicated by the highest explanatory power of its proxy variables (e.g., COD and fDOM) for both urban and non-urban rivers. In the non-urban rivers, N-related indicators were interpreted as primary predictors of CH_4 saturation (e.g., in mixed and agricultural rivers). This relation can be explained given that N contents in the water column could be indicative of the availability of decomposable organic matter in rivers, which were influenced by intensive agricultural production and other land use activities (Renwick et al. 2018). In the forested rivers, DO explains the largest variations in CH_4, underscoring that lotic methanogenesis is anaerobic (Stanley et al. 2016).

The overall explanatory power of multiple linear regressions of CO_2 saturation showed that the highest and lowest R^2 were reported in the urban and forested rivers, respectively. Among all the rivers, CO_2 saturation is primarily explained by water temperature and conductivity. The temperature dependence of CO_2 efflux across rivers is expected, as carbon dioxide (CO_2) is the major end-product of temperature-dependent respiration (Stanley et al. 2016). But there is an exception in forested rivers, where Chl-a was interpreted as the main control. This may be due to the strong collinear between Chl-a and temperature (see Fig. 4) and Chl-a's better explanatory power. NH_4-N also was included as a variable of CO_2 prediction. Rather than considering this substance as an influential factor, NH_4-N may be another byproduct of organic matter mineralization, which theoretically can be collinear with CO_2. Thus, the main mechanism behind CO_2 production across rivers is temperature-dependent with a suitable environment that allows the rapid

decomposition of organic matter.

4.2 Urban river are hotspots of diffusive GHG emissions

Differing results observed among rivers from the Chaohu Lake basin highlight the significance of GHG emissions from urban rivers. The mean estimated N_2O, CH_4, and CO_2 fluxes from the urban rivers reached 471 μmol m^{-2} d^{-1}, 7.1 mmol m^{-2} d^{-1}, and 895.7 mmol m^{-2} d^{-1}, which are nearly 14, seven and two times of those from the non-urban rivers, respectively. Significantly higher GHG fluxes from urban rivers have also been previously documented. Hu et al. (2018) compared GHG fluxes from the Haihe River basin of China and concluded that the N_2O, CH_4, and CO_2 fluxes in sewage-draining urban rivers were almost 1.1-3.1, 3.1-10.9, and 1.2-2.4 times those of other rivers. Wang et al. (2018) and He et al. (2017) found that river networks within the highly urbanized regions commonly emitted the largest areal GHG emissions, with values of 590 μmol m^{-2} d^{-1}, 3.6 mmol m^{-2} d^{-1}, and 873 mmol m^{-2} d^{-1} for riverine N_2O, CH_4, and CO_2 fluxes, corresponding to 13, 12 and 6 times of those reported in less urbanized rivers, respectively. Similarly, Cotovicz et al. (2016) found that CH_4 fluxes in the urban-impacted coastal bay in Brazil can reach 4.8 mmol m^{-2} d^{-1}, a value of 12 times higher than a nearby forested bay. The compiled datasets as shown in Table 1S further showed that mean GHG fluxes reported in worldwide urban rivers were generally < 600 μmol m^{-2} d^{-1} for N_2O, < 6 mmol m^{-2} d^{-1} for CH_4, and < 900 mmol m^{-2} d^{-1} for CO_2, respectively, though wide ranges of variation were also presented (see Table 1S for details). Evidently, our estimations were quite close to these upper limits, indicating comparably higher GHG emissions from the urban

rivers here. This may be attributable to high population density locally and low sewage treatment rates (Huang et al. 2018), which could consistently result in high GHG emissions.

Considering the landscapes that river drained, it is clear that the fluxes of each gas at each watershed were significantly related to the percentage of urban area included (see Fig. 7). However, the parallel analysis using a percentage of agricultural land as an independent variable failed to show similar relationships ($p>0.05$). This information, along with the GHG hotspots that were frequently identified in urban sampled sites, implies that urban rivers are likely GHG emission hotspots.

Several factors lead to significantly high GHG in urban rivers. Urban rivers usually receive substantial nutrients inputs from various sources, which can provide desirable environmental conditions for in-stream GHG production. It has been well documented that most of the processes that favor GHG production—such as nitrification, denitrification, and methanogenesis—usually prefer a low DO environment (Cotovicz et al. 2016, Quick et al. 2019). Enhanced aerobic metabolism of organic matter, which is available due to insufficient sewage treatment and direct domestic discharges, may rapidly deplete DO in the water column, creating suboxic environments that are suitable for biogenic production. Low DO could also be enhanced by damming urban rivers, which would reduce the influx of DO from the atmosphere due to the attenuated flow rates (see Table 1). In addition to suitable DO, adequate supplies of nutrients in urban rivers also motivate microbial metabolisms as

well as mitigate their resource competitions. Schade et al. (2016) documented significant resource competition between denitrifiers and methanogens in headwater streams, but this is unlikely to occur in nutrient-enriched urban rivers. Evidence for that can be found in significantly positive relationships between N_2O and CH_4 saturation in urban rivers (see Fig. 4). The considerable presence of some specific substances in urban rivers can prevent the rapid depletion of dissolved GHG. Hydrogen sulfide (H_2S), one of these substances, has been documented as an important inhibitor of critical enzyme activity (such as nitrous oxide reductase) and some organisms involved in converting GHG (Dalsgaard et al. 2014, Quick et al. 2019). In aggregate, high availability of nutrients and desirable DO levels favor GHG production, while some substances inhibit their subsequent depletion in the water column.

Urban rivers may also receive external GHG fluxes from sewage. Direct measurements of wastewater treatment plant (WWTP) effluent showed that the concentrations for N_2O and CH_4 typically lay within 1200–3300 nmol L^{-1} (Beaulieu et al. 2010) and 0.01–1.06 μmol L^{-1} (Wang et al. 2011), respectively, which is generally higher than the direct measurements in rivers (see Fig. 2). Similarly, CO_2 concentrations in the final effluent of WWTPs can reach ~30 mmol L^{-1} (Caniani et al. 2019). This suggests that once passed into rivers, WWTP effluent may become an important source of riverine GHG. Moreover, there are also considerable untreated sewage discharges in this basin (Province 2017), which may further increase riverine GHG enrichment. Consequently, the river segments in which significant sewage is

discharged are more likely to become GHG emission hotspots.

Additional factors include urban heat island effects and warm sewages discharged from households and industries. The mean in-situ water temperature of all sampling campaigns for urban rivers was 19.5 ℃, which was roughly 1.0-2.0 ℃ higher than other rivers in the Chaohu Lake basin. Thus, associated organisms and microorganisms could utilize such favorable thermal advantages and produce more GHG.

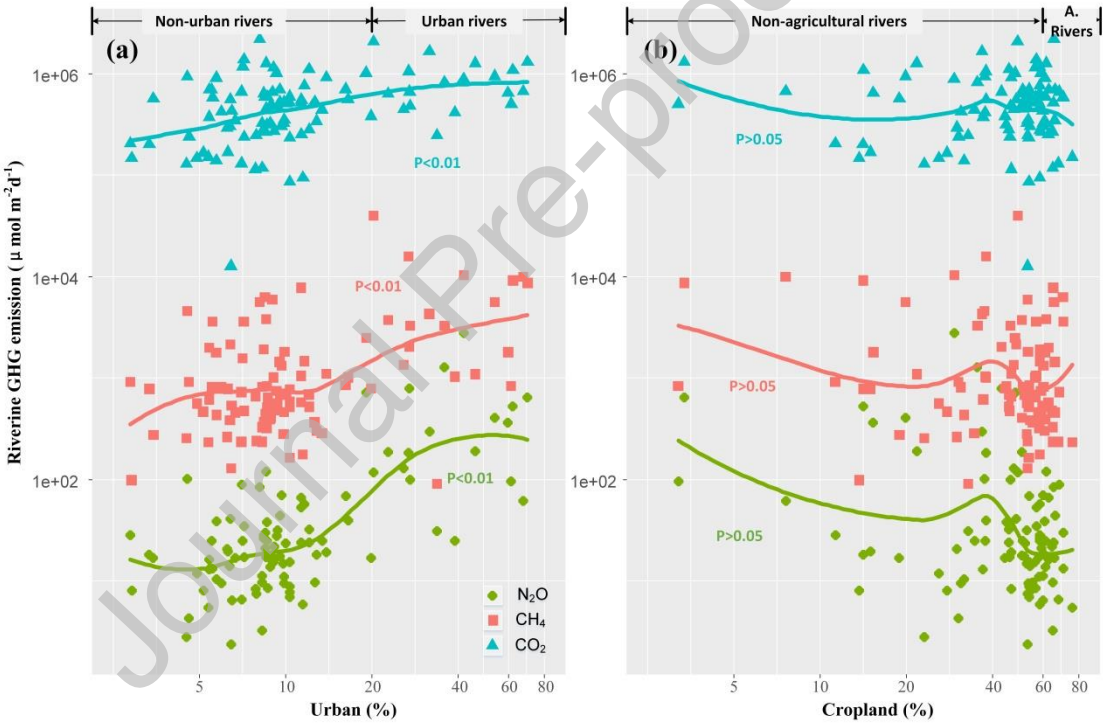

Figure 7. The relationships of mean GHG fluxes from the river reaches between the percentage of a) urban and b) cropland in their drainages, respectively. Locally weighted scatterplot smoothing (LOWESS) fit, as represented by different curves in each subfigure, was used to visually exhibit the impacts of the land cover compositions on GHG fluxes.

4.3 Implications of this study

The global warming potential in the urban rivers rose to 48 g CO_2 m^{-2} d^{-1}, which

was about 1.8~3.4 times of that in the non-urban rivers. Upon further inspection in each sampling campaign, we conclude that, on average, urban rivers always have the highest global warming potential among rivers ($p<0.05$). This underscores that the current IPCC budget accounting of GHG emissions without differentiation between the river types may result in poorly-constrained estimates (IPCC 2019). We encourage regional- and global-scale GHG budget estimates to consider urban rivers more specifically, given that GHG emissions from urban rivers were higher than from other rivers and that urban land cover and populations will continue to expand in the future (Foley et al. 2005).

However, the true level of GHG emissions could be even higher because we only considered diffusive fluxes, while other pathways such as the ebullitive emission (via bubbles) and plant-mediated transport (via the passages in vascular plants) were not included (Stanley et al. 2016). For example, according to Baulch et al. (2011), ebullition was an important pathway of CH_4 emissions, contributing 20%–67% of the total fluxes. Moreover, GHG emissions via ebullition can also be promoted by damming (Maeck et al. 2013, Ran et al. 2017), which is observed in the highly managed Chaohu Lake basin. To comprehensively estimate GHG emissions, therefore, future work should carefully include more in-situ measurement of GHG emissions on rivers and include all emission pathways.

Our estimations have uncertainties. One of the largest uncertainties is derived from our low sampling frequency. The Monte Carlo analysis as shown in the

supplementary material has suggested that finer sampling frequencies can lead to 0.3-5.8% differences in the estimated GHG fluxes (as shown in Table 2S). But the differences could be greater for some specific rivers (see the supplementary material for details). This points to a need for more field measurements with wider spatial coverage and finer frequency to achieve more credible estimations. Another uncertainty is associated with the calculation of *k,* as there are various methods (see details in Raymond et al. (2012)). Here, we adopted equations as proposed by Clough et al. (2007) to calculate *k.* This method considers the influence of wind and water currents, requiring variables such as in-situ temperature, flow rate, wind speed, and riverine width. We obtained all of these data under in-situ conditions to ensure the accurate estimation of *k* and the subsequent robust estimation of GHG fluxes. However, in comparison with other equations, such as Ray01 and Ray05, we found that our estimated fluxes were generally close to those using Ray01 (see the supplementary material). While, Ray01 was more suitable for low-order rivers (Audet et al. 2017), which were not precisely applicable in our case as our monitored rivers were relatively large. In this sense, our choice of the empirical model from Clough et al. (2007) may downplay by ~50% of the GWP if we compared with the Ray05 estimates (see the supplementary material)**.** To assess the accuracy of different calculations of *k* and to obtain more credible estimates, therefore, local measurements of *k* in the hydro-system of the Chaohu Lake Basin are recommended.

5. Conclusions

The main goal of the study was to examine whether urban rivers behave as

regional hotspots of diffusive greenhouse gas (N_2O, CH_4, CO_2) emissions. In this study, we investigated the spatial variability of GHG emissions from different rivers in the mixed-landscape Chaohu Lake basin. Our results demonstrated that urban rivers were the emission hotspots for all greenhouse gases; the mean areal fluxes reached 471.2 ± 1048.8 μmol m^{-2} d^{-1}, 7.1 ± 17.2 mmol m^{-2} d^{-1}, and 895.7 ±780.0 mmol m^{-2} d^{-1}, which were ~14, seven, and two times those from non-urban rivers, respectively. On a CO_2-equivalent basis, the global warming potential in the urban rivers can rise to 48 g CO_2 m^{-2} d^{-1}, which was about 1.8~3.4 times of that in the non-urban rivers. Further stepwise regression revealed why GHG emissions vary significantly across rivers. We concluded that the suboxic conditions with adequate nutrient supply in the water column of urban rivers were the common reasons for higher N_2O and CH_4 emissions, which were in contrast with the aerobic conditions with limited nutrient supply present in the non-urban rivers. The main controls for CO_2 were similar among rivers, which were strongly related to water temperature and conductivity. The urban rivers may have emitted more CO_2 largely because of the high availability of organic matter and physical and chemical conditions that allow rapid decomposition in them. Overall, our studies highlighted the significance of urban rivers in GHG emissions, and corresponding GHG mitigation measures that should be established around these regional hotspots.

Acknowledgments

This study was financially supported by the Thirteenth Five-Year Plan of the Nanjing

Institute of Geography and Limnology (No. NIGLAS2018GH06), the National Natural Science Foundation (No. 41701040, 41877513, 41877487 and 41671479), and the Natural Science Foundation of Jiangsu Province of China (No. BK20171100). We thank Prof. John M Melack from University of California for his insightful suggestions and language edits. We also thank Sanyuan Jiang, Bing Li, Xijun Lai, Zhaoshi Wu, Hui Xie, Fuxiang Zhang, Kaifang Chen, and Lei Zhang from Nanjing Institute of Geography and Limnology for their assistance with field sample collection, laboratory measurements, and data analysis.

Declaration of interests

☒ The authors declare that they have no known competing financial interests or personal relationships that could have appeared to influence the work reported in this paper.

☐The authors declare the following financial interests/personal relationships which may be considered as potential competing interests:

References:

Amaral, J.H.F., Borges, A.V., Melack, J.M., Sarmento, H., Barbosa, P.M., Kasper, D., de Melo, M.L., De Fex-Wolf, D., da Silva, J.S. and Forsberg, B.R. (2018) Influence of plankton metabolism and mixing depth on CO2 dynamics in an Amazon floodplain lake. Science of the Total Environment 630, 1381-1393.

Audet, J., Bastviken, D., Bundschuh, M., Buffam, I., Feckler, A., Klemedtsson, L., Laudon, H., Lofgren, S., Natchimuthu, S., Oquist, M., Peacock, M. and Wallin, M.B. (2020) Forest streams are important sources for nitrous oxide emissions. Global Change Biology 26(2), 629-641.

Audet, J., Wallin, M.B., Kyllmar, K., Andersson, S. and Bishop, K. (2017) Nitrous oxide emissions from streams in a Swedish agricultural catchment. Agriculture Ecosystems & Environment 236, 295-303.

Baulch, H.M., Dillon, P.J., Maranger, R. and Schiff, S.L. (2011) Diffusive and ebullitive transport of methane and nitrous oxide from streams: Are bubble-mediated fluxes important? Journal of Geophysical Research: Biogeosciences 116(G4).

Beaulieu, J.J., Shuster, W.D. and Rebholz, J.A. (2010) Nitrous Oxide Emissions from a Large, Impounded River: The Ohio River. Environmental Science & Technology 44(19), 7527-7533.

Borges, A.V., Abril, G., Darchambeau, F., Teodoru, C.R., Deborde, J., Vidal, L.O., Lambert, T. and Bouillon, S. (2015a) Divergent biophysical controls of aquatic CO2 and CH4 in the World's two largest rivers. Scientific Reports 5(1), 15614.

Borges, A.V., Darchambeau, F., Lambert, T., Bouillon, S., Morana, C., Brouyere, S., Hakoun, V., Jurado, A., Tseng, H.C., Descy, J.P. and Roland, F.A.E. (2018) Effects of agricultural land use on fluvial carbon dioxide, methane and nitrous oxide concentrations in a large European river, the Meuse (Belgium). Science of the Total Environment 610, 342-355.

Borges, A.V., Darchambeau, F., Lambert, T., Morana, C., Allen, G.H., Tambwe, E., Toengaho Sembaito, A., Mambo, T., Nlandu Wabakhangazi, J., Descy, J.P., Teodoru, C.R. and Bouillon, S. (2019) Variations in dissolved greenhouse gases (CO2, CH4, N2O) in the Congo River network overwhelmingly driven by fluvial-wetland connectivity. Biogeosciences 16(19), 3801-3834.

Borges, A.V., Darchambeau, F., Teodoru, C.R., Marwick, T.R., Tamooh, F., Geeraert, N., Omengo, F.O., Guerin, F., Lambert, T., Morana, C., Okuku, E. and Bouillon, S. (2015b) Globally significant greenhouse-gas emissions from African inland waters. Nature Geoscience 8(8), 637-644.

Caniani, D., Caivano, M., Pascale, R., Bianco, G., Mancini, I.M., Masi, S., Mazzone, G., Firouzian, M. and Rosso, D. (2019) CO2 and N2O from water resource recovery facilities: Evaluation of emissions from biological treatment, settling, disinfection, and receiving water body. Science of the Total Environment 648, 1130-1140.

Clough, T.J., Buckthought, L.E., Kelliher, F.M. and Sherlock, R.R. (2007) Diurnal fluctuations of dissolved nitrous oxide (N2O) concentrations and estimates of N2O emissions from a spring-fed river: implications for IPCC methodology. Global Change Biology 13(5), 1016-1027.

Cole, J.J., Prairie, Y.T., Caraco, N.F., McDowell, W.H., Tranvik, L.J., Striegl, R.G., Duarte, C.M., Kortelainen, P., Downing, J.A., Middelburg, J.J. and Melack, J. (2007) Plumbing the Global Carbon Cycle: Integrating Inland Waters into the Terrestrial Carbon Budget. Ecosystems 10(1), 172-185.

Convey, P. and Peck, L.S. (2019) Antarctic environmental change and biological responses. Science Advances 5(11), eaaz0888.

Cotovicz, L.C., Jr., Knoppers, B.A., Brandini, N., Poirier, D., Costa Santos, S.J. and Abril, G. (2016) Spatio-temporal variability of methane (CH4) concentrations and diffusive fluxes from a tropical coastal embayment surrounded by a large urban area (Guanabara Bay, Rio de Janeiro, Brazil). Limnology and Oceanography 61, S238-S252.

Cunada, C.L., Lesack, L.F.W. and Tank, S.E. (2018) Seasonal Dynamics of Dissolved Methane in Lakes of the Mackenzie Delta and the Role of Carbon Substrate Quality. Journal of Geophysical Research: Biogeosciences 123(2), 591-609.

Dalsgaard, Nielsen, L.P., Brotas, V., Viaroli, P., Underwood, G.J.C., Nedwell, D.B., Sundback, K., Rysgaard, S., Miles, A. and Bartoli, M. (2000) Protocol Handbook for Nitrogen Cycling in Estuaries, National Environmental Research Institute, Silkeborg, Denmark.

Dalsgaard, T., Stewart, F.J., Thamdrup, B., De Brabandere, L., Revsbech, N.P., Ulloa, O., Canfield, D.E. and DeLong, E.F. (2014) Oxygen at Nanomolar Levels Reversibly Suppresses Process Rates and Gene Expression in Anammox and Denitrification in the Oxygen Minimum Zone off Northern Chile. Mbio 5(6), 1-14.

Davidson, T.A., Audet, J., Svenning, J.-C., Lauridsen, T.L., Søndergaard, M., Landkildehus, F., Larsen,

S.E. and Jeppesen, E. (2015) Eutrophication effects on greenhouse gas fluxes from shallow-lake mesocosms override those of climate warming. Global Change Biology 21(12), 4449-4463.

Foley, J.A., DeFries, R., Asner, G.P., Barford, C., Bonan, G. and Carpenter, S.R. (2005) Global Consequences of Land Use. Science 309(5734), 570-574.

Harrison, J.A., Matson, P.A. and Fendorf, S.E. (2005) Effects of a diel oxygen cycle on nitrogen transformations and greenhouse gas emissions in a eutrophied subtropical stream. Aquatic Sciences 67(3), 308-315.

He, Y.X., Wang, X.F., Chen, H., Yuan, X.Z., Wu, N., Zhang, Y.W., Yue, J.S., Zhang, Q.Y., Diao, Y.B. and Zhou, L.L. (2017) Effect of watershed urbanization on N2O emissions from the Chongqing metropolitan river network, China. Atmospheric Environment 171, 70-81.

Hu, B.B., Wang, D.Q., Zhou, J., Meng, W.Q., Li, C.W., Sun, Z.B., Guo, X. and Wang, Z.L. (2018) Greenhouse gases emission from the sewage draining rivers. Science of the Total Environment 612, 1454-1462.

Huang, J., zhang, y., Huang, Q. and Gao, J. (2018) When and where to reduce nutrient for controlling harmful algal blooms in large eutrophic lake Chaohu, China? Ecological Indicators 89.

Humborge, C., MÖrth, C.-m., Sundbom, M., Borg, H., Blenckner, T., Giesler, R. and Ittekkot, V. (2010) CO2 supersaturation along the aquatic conduit in Swedish watersheds as constrained by terrestrial respiration, aquatic respiration and weathering. Global Change Biology 16(7), 1966-1978.

IPCC (2014) Climate Change 2014: Synthesis Report. Contribution of Working Groups I, II and III to the Fifth Assessment Report of the Intergovernmental Panel on Climate Change Rep. IPCC, Geneva, Switzerland, pp. 87.

IPCC (2018) Summary for policymakers. In: Global Warming of 1.5°C. Organization, W.M. (ed), Geneva, Switzerland.

IPCC (2019) 2019 Refinement to the 2006 IPCC Guidelines for National Greenhouse Gas Inventories, Volum 4, Chapter 11, edited by: Calvo Buendia, E., Tanabe, K., Kranjc, A., Baasansuren, J., Fukuda, M., Ngarize S., Osako, A., Pyrozhenko, Y., Shermanau, P. and Federici, S., IPCC, Switzerland, Kanagawa, JAPAN.

Iurii, S., Neville, M. and G Philip, R. (2014) Global metaanalysis of the nonlinear response of soil nitrous oxide (N2O) emissions to fertilizer nitrogen. Proceedings of the National Academy of Sciences of the United States of America 111(25), 9199.

Jähne, B., Heinz, G. and Dietrich, W. (1987) Measurement of the diffusion coefficients of sparingly soluble gases in water. Journal of Geophysical Research: Oceans 92(C10), 10767-10776.

Jana, M. and Sar, N. (2016) Modeling of hotspot detection using cluster outlier analysis and Getis-Ord Gi* statistic of educational development in upper-primary level, India. Modeling Earth Systems & Environment 2(2), 1-10.

Ji, Q., Babbin, A.R., Jayakumar, A., Oleynik, S. and Ward, B.B. (2015) Nitrous oxide production by nitrification and denitrification in the Eastern Tropical South Pacific oxygen minimum zone. Geophysical Research Letters 42(24), 10,755-710,764.

Jin, H., Yoon, T.K., Begum, M.S., Lee, E.-J., Oh, N.-H., Kang, N. and Park, J.-H. (2018) Longitudinal discontinuities in riverine greenhouse gas dynamics generated by dams and urban wastewater. Biogeosciences 15(20), 6349-6369.

Laini, A., Bartoli, M., Castaldi, S., Viaroli, P., Capri, E. and Trevisan, M. (2011) Greenhouse gases (CO2, CH4 and N2O) in lowland springs within an agricultural impacted watershed (Po River Plain, northern Italy). Chemistry and Ecology 27(2), 177-187.

Li, L., Chen, H., Zhu, Y., Wang, Y.H. and Ye, J.F. (2020) Relationship Between CO2 and CH4 Emissions in Urban Rivers and Sewage Discharging from a Municipal Drainage Network. 41(7), 3392-3401.

Liu, T.-T., Wang, X.-F., Yuan, X.-Z., Gong, X.-J. and Hou, C.-L. (2019) Spatial-temporal Characteristics and Driving Factors of Greenhouse Gas Emissions from Rivers in a Rapidly Urbanizing Area. Huan jing ke xue= Huanjing kexue 40(6), 2827-2839.

Maeck, A., Delsontro, T., McGinnis, D.F., Fischer, H., Flury, S., Schmidt, M., Fietzek, P. and Lorke, A. (2013) Sediment trapping by dams creates methane emission hot spots. Environ Sci Technol 47(15), 8130-8137.

Marescaux, A., Thieu, V. and Garnier, J. (2018) Carbon dioxide, methane and nitrous oxide emissions from the human-impacted Seine watershed in France. Science of the Total Environment 643, 247-259.

Melack, J.M., Hess, L.L., Gastil, M., Forsberg, B.R., Hamilton, S.K., Lima, I.B.T. and Novo, E.M.L.M. (2004) Regionalization of methane emissions in the Amazon Basin with microwave remote sensing. Global Change Biology 10(5), 530-544.

MEP (2002) Environmental Quality Standards for Surface Water (GB 3838-2002), China Environmental Science Press, Beijing.

Mitchell, A. (2005) The ESRI Guide to GIS analysis, Volume 2: Spatial Measurements and Statistics, Esri Press, Redlands, CA.

Mwanake, R.M., Gettel, G.M., Aho, K.S., Namwaya, D.W., Masese, F.O., Butterbach-Bahl, K. and Raymond, P.A. (2019) Land use, not stream order, controls N2O concentration and flux in the upper Mara River basin, Kenya. Journal of Geophysical Research: Biogeosciences 124, 3491-3506.

Nelson, T.A. and Boots, B. (2010) Detecting spatial hot spots in landscape ecology. Ecography 31(5), 556-566.

Outram, F.N. and Hiscock, K.M. (2012) Indirect Nitrous Oxide Emissions from Surface Water Bodies in a Lowland Arable Catchment: A Significant Contribution to Agricultural Greenhouse Gas Budgets? Environmental Science & Technology 46(15), 8156-8163.

Peterson, B.J., Wollheim, W.M., Mulholland, P.J., Webster, J.R., Meyer, J.L., Tank, J.L., Martí, E., Bowden, W.B., Valett, H.M., Hershey, A.E., McDowell, W.H., Dodds, W.K., Hamilton, S.K., Gregory, S. and Morrall, D.D. (2001) Control of Nitrogen Export from Watersheds by Headwater Streams. Science 292(5514), 86-90.

Province, E.P.D.o.A. (2017) The thirteen five-year plan on water pollution prevention from Chaohu watershed (available at: http://aqxxgk.anqing.gov.cn/show.php?id=588034, access date: 20200713).

Qin, X., Li, Y., Wan, Y., Fan, M., Liao, Y., Li, Y., Wang, B. and Gao, Q. (2020) Diffusive flux of CH4 and N2O from agricultural river networks: Regression tree and importance analysis. Sci Total Environ 717, 137244.

Quick, A.M., Reeder, W.J., Farrell, T.B., Tonina, D., Feris, K.P. and Benner, S.G. (2019) Nitrous oxide from streams and rivers: A review of primary biogeochemical pathways and environmental variables. Earth-Science Reviews 191, 224-262.

Ran, L., Li, L., Tian, M., Yang, X., Yu, R., Zhao, J., Wang, L. and Lu, X.X. (2017) Riverine CO2 emissions in the Wuding River catchment on the Loess Plateau: Environmental controls and dam impoundment impact. Journal of Geophysical Research-Biogeosciences 122(6), 1439-1455.

Raymond, P.A., Hartmann, J., Lauerwald, R., Sobek, S., McDonald, C., Hoover, M., Butman, D., Striegl, R., Mayorga, E., Humborg, C., Kortelainen, P., Durr, H., Meybeck, M., Ciais, P. and Guth, P. (2013) Global carbon dioxide emissions from inland waters. Nature 503(7476), 355-359.

Raymond, P.A., Zappa, C.J., Butman, D., Bott, T.L., Potter, J., Mulholland, P., Laursen, A.E., McDowell, W.H. and Newbold, D. (2012) Scaling the gas transfer velocity and hydraulic geometry in streams and small rivers. Limnology and Oceanography: Fluids and Environments 2(1), 41-53.

Reay, D.S., Davidson, E.A., Smith, K.A., Smith, P., Melillo, J.M., Dentener, F. and Crutzen, P.J. (2012) Global agriculture and nitrous oxide emissions. Nature Climate Change 2(6), 410-416.

Renwick, W.H., Vanni, M.J., Fisher, T.J. and Morris, E.L. (2018) Stream Nitrogen, Phosphorus, and Sediment Concentrations Show Contrasting Long-term Trends Associated with Agricultural Change. Journal of Environmental Quality 47(6), 1513-1521.

Schade, J.D., Bailio, J. and McDowell, W.H. (2016) Greenhouse gas flux from headwater streams in New Hampshire, USA: Patterns and drivers. Limnology and Oceanography 61, S165-S174.

Smith, R.M., Kaushal, S.S., Beaulieu, J.J., Pennino, M.J. and Welty, C. (2017) Influence of infrastructure on water quality and greenhouse gas dynamics in urban streams. Biogeosciences 14(11), 2831-2849.

Sobek, S., Tranvik, L.J. and Cole, J.J. (2005) Temperature independence of carbon dioxide supersaturation in global lakes. Global Biogeochemical Cycles 19(2).

Stanley, E.H., Casson, N.J., Christel, S.T., Crawford, J.T., Loken, L.C. and Oliver, S.K. (2016) The ecology of methane in streams and rivers: patterns, controls, and global significance. Ecological Monographs 86(2), 146-171.

Teodoru, C.R., Nyoni, F.C., Borges, A.V., Darchambeau, F., Nyambe, I. and Bouillon, S. (2015) Dynamics of greenhouse gases (CO2, CH4, N2O) along the Zambezi River and major tributaries, and their importance in the riverine carbon budget. Biogeosciences 12(8), 2431-2453.

Tian, L., Cai, Y. and Akiyama, H. (2019) A review of indirect N2O emission factors from agricultural nitrogen leaching and runoff to update of the default IPCC values. Environmental Pollution 245, 300-306.

Turner, P.A., Griffis, T.J., Baker, J.M., Lee, X., Crawford, J.T., Loken, L.C. and Venterea, R.T. (2016) Regional-scale controls on dissolved nitrous oxide in the Upper Mississippi River. Geophysical Research Letters 43(9), 4400-4407.

Turner, P.A., Griffis, T.J., Lee, X.H., Baker, J.M., Venterea, R.T. and Wood, J.D. (2015) Indirect nitrous oxide emissions from streams within the US Corn Belt scale with stream order. Proceedings of the National Academy of Sciences of the United States of America 112(32), 9839-9843.

Venkiteswaran, J.J., Rosamond, M.S. and Schiff, S.L. (2014) Nonlinear response of riverine N2O fluxes to oxygen and temperature. Environ Sci Technol 48(3), 1566-1573.

Wallin, M.B., Löfgren, S., Erlandsson, M. and Bishop, K. (2014) Representative regional sampling of carbon dioxide and methane concentrations in hemiboreal headwater streams reveal underestimates in less systematic approaches. Global Biogeochemical Cycles 28(4), 465-479.

Wang, J., Zhang, J., Xie, H., Qi, P., Ren, Y. and Hu, Z. (2011) Methane emissions from a full-scale A/A/O wastewater treatment plant. Bioresource Technology 102(9), 5479-5485.

Wang, J.N., Chen, N.W., Yan, W.J., Wang, B. and Yang, L.B. (2015) Effect of dissolved oxygen and nitrogen on emission of N2O from rivers in China. Atmospheric Environment 103, 347-356.

Wang, R., Zhang, H., Zhang, W., Zheng, X., Butterbach-Bahl, K., Li, S. and Han, S. (2020) An urban

polluted river as a significant hotspot for water–atmosphere exchange of CH4 and N2O. Environmental Pollution 264, 114770.

Wang, X., He, Y., Chen, H., Yuan, X., Peng, C., Yue, J., Zhang, Q. and Zhou, L. (2018) CH4 concentrations and fluxes in a subtropical metropolitan river network: Watershed urbanization impacts and environmental controls. Science of the Total Environment 622, 1079-1089.

Wanninkhof, R. (1992) Relationship between wind speed and gas exchange over the ocean. Journal of Geophysical Research Oceans 97(C5), 7373-7382.

Weiss, R.F. (1974) Carbon dioxide in water and seawater: the solubility of a non-ideal gas. Marine Chemistry 2(3), 203-215.

Weiss, R.F. and Price, B.A. (1980) Nitrous oxide solubility in water and seawater. Marine Chemistry 8(4), 347-359.

Wiesenburg, D.A. and Guinasso, N.L. (1979) Equilibrium solubilities of methane, carbon monoxide, and hydrogen in water and sea water. Journal of Chemical & Engineering Data 24(4), 356-360.

Wilcock, R.J. and Sorrell, B.K. (2008) Emissions of greenhouse gases CH4 and N2O from low-gradient streams in agriculturally developed catchments. Water Air and Soil Pollution 188(1-4), 155-170.

WMO (2019) WMO greenhouse gas bulletin : the state of greenhouse gases in the atmosphere based on global observations through 2018, Global Atmosphere Watch, World Meteorological Organization.

Wrage, N., Velthof, G.L., van Beusichem, M.L. and Oenema, O. (2001) Role of nitrifier denitrification in the production of nitrous oxide. Soil Biology and Biochemistry 33(12), 1723-1732.

Xia, Y., Li, Y., Ti, C., Li, X., Zhao, Y. and Yan, X. (2013) Is indirect N2O emission a significant contributor to the agricultural greenhouse gas budget? A case study of a rice paddy-dominated agricultural watershed in eastern China. Atmospheric Environment 77, 943-950.

Xiao, Q., Duan, H., Qi, T., Hu, Z., Liu, S., Zhang, M. and Lee, X. (2020) Environmental investments decreased partial pressure of CO2 in a small eutrophic urban lake: Evidence from long-term measurements. Environ Pollut 263(Pt A), 114433.

Yang, D., Mao, X., Wei, X., Tao, Y., Zhang, Z. and Ma, J. (2020) Water–Air Interface Greenhouse Gas Emissions (CO2, CH4, and N2O) Emissions Were Amplified by Continuous Dams in an Urban River in Qinghai–Tibet Plateau, China. Water 12(3).

Yu, Z.J., Deng, H.G., Wang, D.Q., Ye, M.W., Tan, Y.J., Li, Y.J., Chen, Z.L. and Xu, S.Y. (2013) Nitrous oxide emissions in the Shanghai river network: implications for the effects of urban sewage and IPCC methodology. Global Change Biology 19(10), 2999-3010.

Yvon-Durocher, G., Allen, A.P., Bastviken, D., Conrad, R., Gudasz, C., St-Pierre, A., Thanh-Duc, N. and del Giorgio, P.A. (2014) Methane fluxes show consistent temperature dependence across microbial to ecosystem scales. Nature 507(7493), 488-491.

Zhang, W., Li, H. and Li, Y. (2019) Spatio-temporal dynamics of nitrogen and phosphorus input budgets in a global hotspot of anthropogenic inputs. Science of The Total Environment 656, 1108-1120.

Zhang, W., Li, H., Xiao, Q., Jiang, S. and Li, X. (2020) Surface nitrous oxide (N2O) concentrations and fluxes from different rivers draining contrasting landscapes: Spatio-temporal variability, controls, and implications based on IPCC emission factor. Environmental Pollution 263, 114457.

Table 1. Statistical characteristics of riverine physical and chemical indicators.

Indicators	Unit	Urban	Mixed	Agri	Forest
TN		**7.68±4.26** [a*]	2.15±1.65 [b]	2.51±3.3 [b]	1.72±0.92 [c]
NO_3-N		**2.30±1.80** [a]	0.79±0.81 [b]	0.75±0.72 [b]	1.01±0.79 [b]
NO_2-N		**0.46±0.86** [a]	0.07±0.23 [b]	0.042±0.07 [b]	0.040±0.08 [b]
NH_4-N	mg L^{-1}	**3.31±3.78** [a]	0.45±0.90 [b]	0.41±0.65 [b]	0.17±0.24 [b]
TP		**0.50±0.44** [a]	0.16±0.22 [b]	0.16±0.19 [b]	0.11±0.08 [b]
COD		5.57±2.16 [ab]	4.84±1.83 [b]	**6.69±10.44** [a]	3.20±1.32 [b]
DO		6.37±3.20 c	8.88±3.12 [ab]	8.77±3.66 [b]	**9.66±2.6** [a]
pH	-	8.02±0.53 [b]	8.17±0.79 [ab]	8.24±0.78 [a]	**8.33±0.68** [a]
SPC	ms cm^{-1}	**0.72±0.49** [a]	0.42±0.25 [b]	0.35±0.20 c	0.20±0.13 [d]
ORP	mV	184.10±39.87 [a]	**191.09±55.47** [a]	181.65±51.31 [a]	182.39±51.69 [a]
Turbidity	FNU	50.84±80.45 [a]	**97.27±707.01** [a]	63.47±163.28 [a]	15.67±26.55 [a]
fDOM	ppb	**48.08±18.59** [a]	38.76±19.60 [b]	40.10±18.44 [ab]	21.05±14.08 [b]
Chl-a	ug L^{-1}	**13.47±23.49** [a]	7.29±10.53 [b]	8.17±9.83 [b]	3.11±7.38 [c]
Riverine width	m	59.63±31.83 [a]	**81.53±150.17** [a]	39.66±28.63 [b]	51.02±51.75 [a]
Mean depth		1.39±0.99 [b]	**1.54±0.95** [a]	1.03±0.48 [b]	1.25±0.88 [b]
Mean flow rate	m s^{-1}	0.06±0.09 [b]	0.11±0.28 [a]	0.12±0.30 [a]	**0.15±0.18** [a]

* All of the data were shown as Mean±SD. Note that the affiliated letters a, b, c, and d indicate statistical differences at the 95% confidence level among rivers.

Table 2. Diffusive emissions of greenhouse gases and their CO_2-equivalent fluxes from different rivers.

River types	N_2O	CH_4	CO_2	CO_2-equivalent fluxes
	μmol m^{-2} d^{-1}	mmol m^{-2} d^{-1}		g CO_2 m^{-2} d^{-1}
Urban rivers	471.2±1048.8	7.1±17.2	895.7±780.0	48.1±39.3
Non-urban Rivers	34.3±131.3	1.2±3.2	501.4±520.3	23.0±23.5
Mixed rivers	41.9±181.8	1.0±2.2	581.0±512.9	26.5±23.0
Agricultural rivers	34.8±74.0	1.9±4.9	551.4±617.4	25.5±28.2
Forested rivers	20.6±35.7	0.9±1.9	308.9±343.8	14.2±15.6